Design Principles for a Family of Direct-Drive Legged Robots

Gavin Kenneally, Avik De, and D. E. Koditschek

***Abstract*—This letter introduces Minitaur, a dynamically running and leaping quadruped, which represents a novel class of direct-drive (DD) legged robots. We present a methodology that achieves the well-known benefits of DD robot design (transparency, mechanical robustness/efficiency, high-actuation bandwidth, and increased specific power), affording highly energetic behaviors across our family of machines despite severe limitations in specific force. We quantify DD drivetrain benefits using a variety of metrics, compare our machines' performance to previously reported legged platforms, and speculate on the potential broad-reaching value of "transparency" for legged locomotion.**

***Index Terms*—Multilegged Robots, Mechanism Design of Mobile Robots, Novel Actuators for Natural Machine Motion.**

I. Introduction

A DIRECT-DRIVE (DD) robot [1] forgoes the use of a gear, belt, chain, or other reduction to amplify its motors' effective torque production. This is in contrast to other actuation approaches used with electromagnetic motors such as high stiffness, large reduction geartrains typically found in humanoid machines [2], and highly compliant series elastic actuators (SEA) [3]. In this letter we introduce a new class of DD legged platforms and present new design principles that underpin their effective operation[1]. This class includes Minitaur, a quadruped with two active DOF per leg Fig. 1, center); Delta Hopper, a monoped with three active DOF per leg Fig. 1, left); and Penn Jerboa, a tailed biped with one active DOF/leg, and compliant C-shaped legs Fig. 1, right) [5]. These three robots share a common electromechanical infrastructure, demonstrating that the design principles detailed below can be successfully instantiated in very different morphologies.

A. Motivation

Our interest in DD architecture is motivated by a number of specific benefits first understood in the context of manipulation [1]. We review how the DD paradigm presents advantages (and disadvantages) in the context of legged locomotion.

1) DD Advantages for Legged Locomotion:

a) Transparency: DD actuation benefits robotics applications by avoiding backlash, achieving high mechanical stiffness, and mitigating reflected inertia of the motor and coulomb and viscous friction in the gearbox so that motor dynamics can be more quickly and easily influenced by external forces acting on the leg [1].

b) Mechanical performance: Eliminating the gearbox results in improvements in: **mechanical robustness**, since there are no gears to protect from impulses [3], [6]; **dynamic isolation of the body**, since it is only coupled to the legs through the motor's air gap and inertially through the motor's bearing; **mechanical efficiency**, since DD machines experience no mechanical losses due to gear reduction whereas standard planetary gearboxes have a maximum efficiency of 60–90% [7], and exhibit directional dependency [8]; and **control methodology** since decreased mechanical complexity exposes Lagrangian dynamics, promoting behavioral strategies relying on torque [1], [9], impedance [10], [11], and other "natural" (physically robust and mathematically well-founded) control methods [12].

c) High-bandwidth signal flow: Removing the gearbox enables advantages in: **sensing**, mitigating low-pass spring dynamics arising in SEA [3], as well as filter dynamics in feeding back distal force/torque readings [13] (slowing a 3kHz control loop down to 600Hz in the latter case); **actuation**, since avoiding SEA also removes the low-pass filtering of actuation signals [3]; hence **tunable compliance** can be implemented at kHz timescales, the sort of reactivity known to play an important role in animal negotiation of complex terrain [14].

d) Specific power: Since a gearbox both increases mass and decreases power (because of its associated losses), the peak specific power of DD actuators will be significantly higher than their geared counterparts.

2) DD Disadvantages for Legged Locomotion: Without a gearbox to amplify the output torque and decrease the output speed, DD motors must operate in high-torque, low-speed regimes where Joule heating is significant. This means that the actuators must mostly operate far from both their peak power and peak efficiency, which both occur much closer to no-load speed [7].

B. Contributions and Organization

This letter documents the methodology underlying the design and construction of the first (to our best knowledge) examples

Manuscript received August 31, 2015; accepted January 4, 2016. Date of publication February 11, 2016; date of current version March 4, 2016. This paper was recommended for publication by Associate Editor B. Vanderborght and Editor A. Bicchi upon evaluation of the reviewers comments. This work was supported in part by the NSERC 326008481 and ARL/GDRS RCTA project, Coop. Agreement W911NF-1020016, in part by the U.S. Army Research Laboratory under Cooperative Agreement Number W911NF-10-2-0016, and in part by the National Science and Engineering Research Council of Canada 352093.

G. Kenneally is with the Department of Mechanical Engineering and Applied Mechanics, University of Pennsylvania, Philadelphia, PA 19104-6315 USA (e-mail: gake@seas.upenn.edu).

A. De and D. E. Koditschek is with the Department of Electrical and Systems Engineering, University of Pennsylvania, Philadelphia, PA 19104-6315 USA (e-mail: avik@seas.upenn.edu, kod@seas.upenn.edu).

Digital Object Identifier 10.1109/LRA.2016.2528294

[1]This letter adds substantially new analysis and experimental results to a preliminary announcement originally presented in workshop form [4].

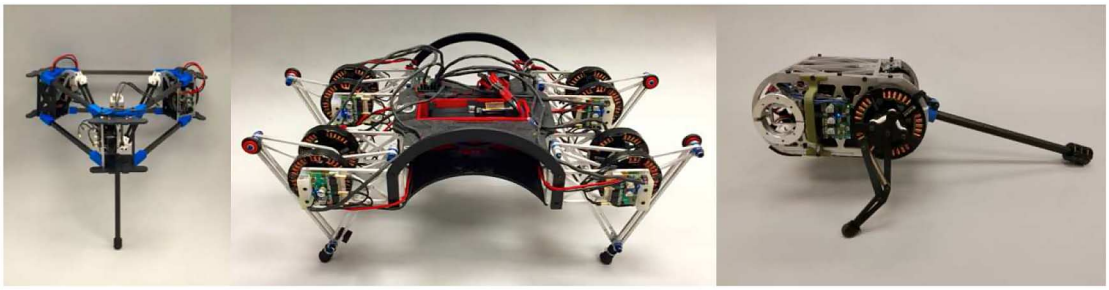

Fig. 1. The DD robots discussed in this letter: Delta Hopper (**left**), Minitaur (**center**), and Jerboa (**right**).

of general-purpose DD legged robots using conventional rotary actuators[2].

The most salient contribution of this letter is a comparative measure, a_{mcv}, (11) that provides a necessary condition governing whether a legged robot (comprised of specific actuators, linkages, and leg configuration, operating at a specific length scale) will be suitable for DD operation. As an important part of this overall robot measure, we identify a new motor sizing measure (2) that exposes a key feature for DD legged locomotion performance. We present a detailed analysis of our five-bar linkage [17] and describe its benefits for both transmission Fig. 5-**B**) and thermal cost Fig. 5-**C**) of force production, addressing directly the two main disadvantages of DD design for legged locomotion. These result in our DD family's competitive locomotion performance as compared to more established geared machines (verified empirically in Table III).

Section II lays out the design methodology, Section III documents the resulting empirical drivetrain performance, Section IV reports on some of the locomotive consequences, and the letter concludes with a brief appraisal and glimpse at future work in Section V.

II. Design

Gear ratios in legged robots are typically in the range of 20:1 to 300:1 [18]–[21], so by removing the gearbox, mass-specific torque (not power) becomes the first limiting resource in electromagnetically actuated robots [1], [9]. Adopting the perspective of locomotion as self-manipulation [22], the force/torque resource becomes even more scarce as the machine's payload must now include the robot mass itself. In addition to the limited specific force, the diminished electromechanical efficiency near stall conditions makes DD operation potentially energetically expensive.

The design problems associated with actuator selection, configuration, recruitment, and leg kinematics must therefore address one central theme, namely how to mitigate the specific force scarcity.

A. Actuator Selection

In the DD family, motors are selected to maximize specific torque at two time scales: **instantaneous performance** (peak specific torque) limited by flux saturation of the motor's core, and **steady performance** (thermal specific torque) limited by the winding enamel's maximum temperature.

[2]The possible exceptions are very specialized (not general-purpose) machines [15], and those using custom DD linear actuators [16].

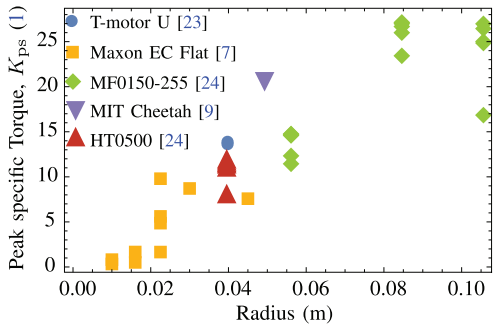

Fig. 2. Peak specific torque (limited by flux saturation; affects instantaneous performance) against gap radius for a selection of legged robot actuators.

Peak specific torque [9],

$$K_{\text{ps}} := \frac{K_t i_p}{m} \qquad (\text{in units of } \tfrac{\text{Nm}}{\text{kg}}), \tag{1}$$

where K_t is the motor's torque constant ($\frac{\text{Nm}}{\text{A}}$), i_p the peak current (A) before the core is flux saturated, and m the motor's mass (kg). Our new metric, thermal specific torque,

$$K_{\text{ts}} := \frac{K_t}{m}\sqrt{\frac{1}{R_{\text{th}}R}}, \qquad (\text{in units of } \tfrac{\text{Nm}}{\text{kg}\sqrt{^\circ\text{C}}}), \tag{2}$$

where R_{th} is the motor's thermal resistance (in units of $^\circ$C/W), and R is its electrical resistance (in Ω), conveys a motor's desirable ability to produce torque at stall in contrast with its production and dissipation of waste thermal energy caused by Joule heating. Thermal specific torque is similar to the dimensionless motor constant K_m (in units of $\frac{\text{N m}}{\sqrt{W}}$) [1] and is also winding invariant [17] but takes mass and thermal dissipation into account. Generally, this measure is tied favorably to the motor's gap radius [9] resulting in better performance for outrunners (rotor on the outside) compared to inrunners (rotor on the inside), and motors with a large radius to depth ratio [1].

Figs. 2 and 3 show plots of K_{ps} and K_{ts} (respectively) against gap radius for a variety of motors, many of which are used in the state of the art machines listed in Table II, whose motors are specified in Footnote 9.

The plot of peak specific force against gap radius, r, in Fig. 2 demonstrates a very strong linear trend (up to differences in framing mass and magnetic permeability of the core). Thermal specific force Fig. 3 is also quite linear in gap radius, but three

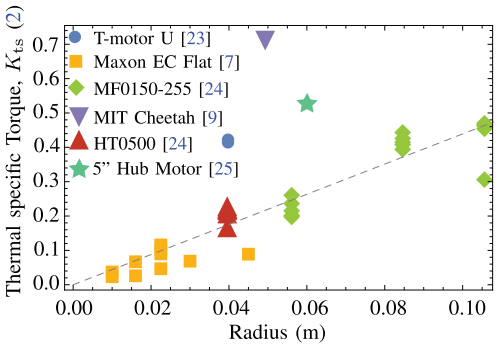

Fig. 3. Thermal specific torque (limited by winding temperature; affects steady-state performance) against gap radius for a selection of legged robot actuators. The dashed line indicates the mean of the "inliers" detailed in Section. II-A.

important outliers become apparent: the 5" hub motor, T-Motor U series (used in this family of machines) and the custom motors made for the MIT Cheetah [26].

The new K_{ts} metric (2) reveals that electromechanical DD design for legged locomotion entails a degree of "inverse motor sizing," whereby the robot's length scale is constrained by the availability of COTS motors with adequately good K_{ts} (such as the outliers noted in Fig. 3 at that scale. That is to say that this is a technological, as opposed to fundamental limitation. Here, the term "adequately good" is governed by the effect of K_{ts} on the continuous thermally sustainable torque in the a_{mcv} measure detailed in (11), which must be positive for the machine to stand indefinitely in the least favorable posture that keeps the toes directly below the hips. Ignoring the three outliers in the K_{ts} plot, a linear fit over the rest of the data gives $K_{\text{ts}} = 4.39\,r$, with a coefficient of determination of 0.895. Using the standard thermal model [7], [27], actuators can incur a core rise of $100\,^{\circ}C$[3], and the robot's design is assumed to achieve an optimistic Table II actuator mass fraction of 40%. Measuring the length of the first link in units of r (gap radius) to cancel the r in the K_{ts} plot, results in $\min(\Gamma_v) = \frac{1}{r}$ (7). For the linear fit of most of the motors, $a_{mcv} \geq 0$ implies the first link must be $\leq 1.79\,r$, whereas the 5" hub motor can be $\leq 3.60\,r$, for the U8 $\leq 4.34\,r$ is possible, and for the MIT Cheetah motors, $\leq 6.02\,r$ can be achieved. In other words, for all these "inliers" (the actuators with aggregate 4.39 slope in Fig. 3), a DD legged platform would be uselessly "stubby" as the majority of the first link length would be consumed by the motor's radius, resulting in minimal usable toe workspace (see Section II-B for more detailed explanation of the workspace of these mechanisms). The MIT Cheetah motors would be very suitable for DD use, but the length scale of the machine would have to decrease significantly compared to the existing Cheetah robot.

B. Actuator Recruitment Via Leg Design

The legs of our DD robot family vary in the number of actuated DOF from one to three, and the legs of the two machines with multiply actuated DOF (Minitaur, Delta Hopper) incorporate closed kinematic chains (linkages). Because of the simpler kinematics, the 2-DOF case is analyzed in detail, comparing a serial chain of two revolute joints, (3), (denoted by "O"), a parallelogram five-bar, (4), (a linkage frequently used in DD robot arms [1], denoted by "P"), and a the symmetric five-bar, (5), used in the Minitaur robot, detailed in [17] (denoted by "S"). The Delta Hopper machine uses the 3-DOF generalization of the 2-DOF symmetric five-bar employed in Minitaur[4]. The Jerboa, however, cannot benefit from such analysis of parallel linkages as it has only has 1-DOF/leg[5].

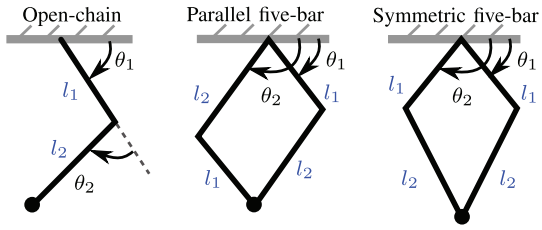

Fig. 4. Leg designs considered in Section II-B.

Given joint angles $q := (\theta_1, \theta_2) \in T^2$ (see Fig. 4), the forward kinematics for the three candidate leg designs are

$$g_O(q) = \mathrm{R}(\theta_1) \begin{bmatrix} l_2 \cos\theta_2 \\ l_1 + l_2 \sin\theta_2 \end{bmatrix}, \tag{3}$$

$$g_P(q) = \mathrm{R}(\alpha_1) \left(l_1 \mathrm{R}(\alpha_2) e_1 + l_2 \mathrm{R}(\alpha_2)^T e_1 \right), \tag{4}$$

$$g_S(q) = \mathrm{R}(-\alpha_1) \begin{bmatrix} 0 \\ l_1 \cos\alpha_2 + \sqrt{{l_2}^2 - {l_1}^2 \sin^2\alpha_2} \end{bmatrix}, \tag{5}$$

where $\mathrm{R} : S^1 \to \mathrm{SO}(2)$ is a rotation matrix, e_i denotes the i^{th} standard basis vector, and the $\alpha_1 := (\theta_1 + \theta_2)/2$, $\alpha_2 := (\theta_1 - \theta_2)/2$ coordinate change (for the parallel designs) enables a helpful factoring of the forward kinematics in each case (cf. Appendix A).

Now, if $J := \mathrm{D}_q g$ is the Jacobian of the forward kinematics, g, the joint velocities $\dot{q}$, (Cartesian) toe velocity $\dot{p}$, joint torques τ, and toe force f satisfy

$$\dot{p} = J\dot{q}, \qquad \tau = J^T f. \tag{6}$$

Additionally, we define the vertical effective mechanical advantage, $\Gamma_v : T^2 \to \mathbb{R}^2$, as

$$\Gamma_v(q) := \begin{bmatrix} 0 & 1 \end{bmatrix} J(q)^{-T}. \tag{7}$$

We compute the singular values of J, σ_i, and then consider standard manipulability measures [28] for each of the candidate mechanism designs. In each case the workspace is generically an annulus, it is fully defined by $r_{\min}$ (the minimum radius)

[3]This somewhat arbitrary criterion reflects our working practice safety margin with our lab's various electromagnetic actuators since the windings typically melt around $140\,^{\circ}C$.

[4]The linkage in Minitaur consists of two RR chains closing at the toe, while the Delta Hopper linkage has three RR chains that close at the toe. Assuming the same choice of link lengths, the leg kinematics in the two machines are very similar, except that the Delta Hopper's workspace is cut off at either extreme end of extension because the actuators cannot be made coaxial.

[5]The Jerboa benefits from the two major design principles embodied by (2) & (11). Its inclusion in the present letter further serves the important role of illustrating that the additional advantage conferred by the symmetric linkage - while beneficial as manifest in the superior load bearing capabilities revealed by the a_{mcv} values of Table III - is not *necessary* to the success of a DD design.

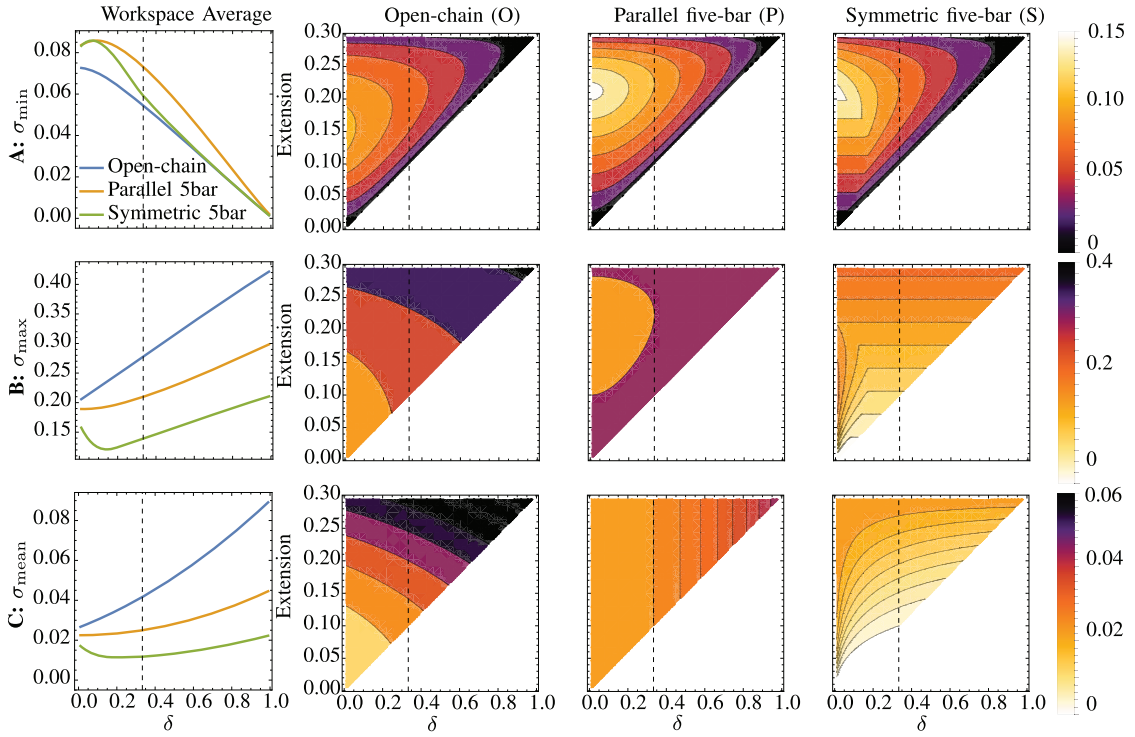

Fig. 5. In each of the subfigures (rows) the first column shows the workspace averaged measure of the particular function of singular values, σ, plotted against the ratio of minimal to maximal leg radius, δ. The remaining three columns provide a more detailed view of the particular σ as a function of both δ and leg extension. **A**: Leg Jacobian minimum singular values Section II-B1: higher values yield greater proprioceptive sensitivity. **B**: Leg Jacobian maximum singular values Section II-B2: lower values indicate better minimum force production. **C**: Leg Jacobian mean singular values Section II-B3: lower values indicate smaller thermal cost of producing force. In each figure, the vertical dashed line indicates the linkage used in the Minitaur leg.

and $r_{\max}$ (the maximum radius). In each of the following subsections, we have fixed a constant $r_{\max}$, and plotted a relevant measure over two axes:

a) the design space, $\delta := \frac{r_{\min}}{r_{\max}}$, where $r_{\min} = |l_1 - l_2|$, $r_{\max} = l_1 + l_2$ and
b) the workspace variable, y representing the radial extension of the leg.[6]

1) $\sigma_{\min} := \min_i \sigma_i$, *Proprioceptive Sensitivity:* This measure indicates the minimal speed of the toe in any direction for given motor angular velocities [28], shown in Fig. 5-**A**. More importantly in our problem domain, a very small $\sigma_{\min}$ indicates that some forces at the toe are barely visible to the motor,

$$\min_{\|f\|=1} \tau^T \tau = \min_{\|f\|=1} f^T J J^T f = \sigma_{\min}^2, \tag{8}$$

and so higher values of $\sigma_{\min}$ are favorable (cf. Appendix B-1). From Fig. 5-**A**, the two parallel mechanisms have better proprioception through a larger portion of their workspace.

2) $\sigma_{\max} := \max_i \sigma_i$, *Force Production:* At non-singular configurations, this measure indicates the worst case force at the end effector for bounded motor torque,

$$\min_{\|\tau\|=1} f^T f = \min_{\|\tau\|=1} \tau^T J^{-1} J^{-T} \tau = \frac{1}{\sigma_{\max}^2}. \tag{9}$$

(cf. Appendix B-2). Intuitively, this expresses the degree to which an arbitrary external force can be resisted by the (torque-limited) actuators, and so lower values of $\sigma_{\max}$ are favorable.

[6]We show in Appendix A that each of these measures is invariant to the leg angle, making the extension the only relevant workspace parameter.

As shown in Fig. 5-**B**, the symmetric five-bar does consistently better than the other two mechanisms, in spite of displaying a greater variation over its workspace.

3) $\sigma_{mean} := \frac{1}{n} \operatorname{trace}(JJ^T)$, *Thermal Cost of Force:* Fixing the motor constant, $K_m = 1$, the thermal cost of force production is a function of the infinitesimal kinematics [1, pg. 55], given in $\frac{Nm}{W}$. As shown in Fig. 5-**C** (note that this measure is also leg-angle-invariant; cf. Appendix B-3), the symmetric five-bar has superior design-averaged performance compared to the parallelogram five-bar and series linkages.

C. Mass Budgeting for Robot-Specific Power and Force

It has long been understood in the legged locomotion design literature that a large fraction of the robot's mass budget should be reserved for actuation [27]. Our desire for DD designs pushes this notion toward its extreme as the robots in this family all have approximately 40% of total mass taken up by the actuators, compared to 24% for the modestly geared MIT Cheetah and approximately 10-15% for more conventional machines (detailed in Table II).

D. Leg Workspace and Infinitesimal Kinematics

In the case of Minitaur and Delta Hopper, by allowing the "knee" joints to operate above the "hip" joints (the aforementioned symmetric five-bar in Minitaur and its three-dimensional extension in Delta Hopper), the workspace is doubled and the infinitesimal kinematics are made more favorable. This results

in a 2.1x increase in energetic output in a single stride from a fixed power source and a 5x decrease in collision losses at touchdown compared to a more conventional design, as described in [17].

E. "Framing" Costs

While increasing the number of active DOF/leg can improve control affordance, distributing actuators incurs inescapable costs (paid in the scarce resource of specific force) associated with replacing a single larger actuator by multiple smaller ones. When considering how a motor's output torque scales as the characteristic length is modified, the designer must decide which motor scaling is more representative of the actuator choices available namely isometrically, or by assuming a constant cross section and varying the gap radius.[7] For a constant actuator mass budget, as the number of actuators, n, increases and the actuators scale isometrically, the specific torque scales as $\propto n^0$ if the motors are added in parallel and $\propto n^{-1}$ if they are in series. If the actuators are instead scaled by gap radius, the specific force goes $\propto n^{-1}$ in parallel and $\propto n^{-2}$ in series.[8] This scaling argument represents the minimal characteristic rate of lost specific force production incurred by adding motors whereas, in practice, the additional motors accrue additional cost arising from the further increment of mass (and complexity) needed to frame and attach them. The machines considered in this letter all have one to three active DOF/leg (see Table II) but humanoids such as Asimo [2] with 57 actuated DOF will incur significant cost.

III. Actuator Transparency and Bandwidth

A simple linear dynamical model (consisting of static, kinetic, and viscous friction, and the actuator's reflected inertia), that is invariant to gear ratio, permits a quantitative comparison between DD and conventional geared design. We thus characterize actuation bandwidth, for just as transparency improves proprioception, high bandwidth is necessary for fast closed-loop response. Finally, these relative advantages in our design are contextualized with respect to the family of machines presented in this work.

A. Transparency Measures

The reflected inertia of the Maxon EC-45 is reported in [7] and then scaled by the gear ratio (23:1 in this case) squared. The T-Motor U8's rotor inertia is over-estimated by assuming that the full mass of the rotor is located in an annular ring bound by the outer and gap radii. The static friction ("stiction") of the two actuators is found by attaching 25 mm radius pulleys onto the output shafts, and adding mass until there is movement. Using the same pulleys, varying masses are attached and allowed to fall for 2m, accelerating the motors. This time series data is fit to a first-order system and the steady speed is extracted in each trial. This experiment is performed at five different steady speeds for each motor (10-200$\frac{rad}{s}$ for the U8 and 5-20$\frac{rad}{s}$ for the EC45) resulting in a strong affine fit (coefficient of determination > 0.995), where the vertical axis intercept and slope are the kinetic ("Coulomb" or "dry") and viscous ("Rayleigh" or "damping") friction coefficients, respectively.

TABLE I
Comparison of Specific Conventional and DD Actuators

	EC45-70W, 23:1	U8
Mass (kg)	0.35	0.25
K_v ($\frac{\text{rev}}{V\text{sec}}$)	0.188	1.67
Continuous Torque (Nm)	2.95	0.855
Peak Torque (Nm)	18.86	3.5
Max Continuous Power @15V (W)	12.18	35.63
Reflected Inertia (kg-m^2)	0.0096	0.0001
Static Friction (Nm)	0.218	0.056
Kinetic Friction (Nm)	0.088	0.023
Viscous Friction ($\frac{Nm}{rad/s}$)	0.0071	0.00013
Backlash (deg)	0.8	0

In each of the three measures shown in Table I, the DD actuator (U8) fared significantly better than the conventional geared alternative (EC-45, 23:1), representing a 96x decrease in reflected inertia, 3.89x decrease in static friction, 3.83x decrease in kinetic friction, and 54.6x decrease in viscous drag. This comes at the price of a 2.5x decrease in continuous and a 5.39x decrease in peak specific torque. We leave the larger issues of this tradeoff to the existing analysis in the prior DD robotics literature [1] because we believe the cost/benefit relationships are general to the field whereas we are specifically focused here, simply on the achievability of DD design for legged locomotion.

B. Reflected Inertia Invariance

If motors are scaled by varying gap radius, r, then torque $\propto r^2$ and inertia $\propto r^3$, and so torque/inertia $\propto \frac{1}{r}$. If the motors are scaled isometrically, inertia goes $\propto r^4$, and torque $\propto r^3$, so once again torque/inertia is $\propto \frac{1}{r}$. Considering a gearbox with gear ratio G, torque goes $\propto G$, reflected inertia $\propto G^2$, and so torque/inertia $\propto \frac{1}{G}$. In both cases, to increase torque (either by choosing a motor with a larger gap radius, or by increasing the gear ratio) the price in terms of increased reflected inertia is the same, giving no advantage to minimal gear ratio or even DD.

C. Actuation Bandwidth

Actuation bandwidth between the two motors of interest (EC45 23:1, and U8) was explored by connecting the motors to a power supply at 12V, and limited to their thermally sustainable currents representing a $100\,^{\circ}C$ rise in steady state (3.25A and 9A respectively). The motors were then commanded

[7]The scaling choice depends on both the design objective and availability of COTS (or feasibility of making custom) actuators.

[8]Assuming constant density, the mass budget yields a volume budget, and so the volume of each actuator, v, will be the total volume budget divided by n, so $n \propto v^{-1}$. Scaling isometrically, mass $\propto l^3$ and torque $\propto l^3$ (as both the gap area and radius contribute to torque production), yielding specific torque $\propto n^0$ in parallel. In series, the torque at the end effector is the minimum of the torques in the chain (assuming constant link lengths), so at best $\propto n^{-1}$. If scaling is done according to gap radius, torque $\propto l^3$ but mass $\propto l^2$ resulting in specific force in parallel $\propto n^{-1}$ and similarly in series $\propto n^{-2}$.

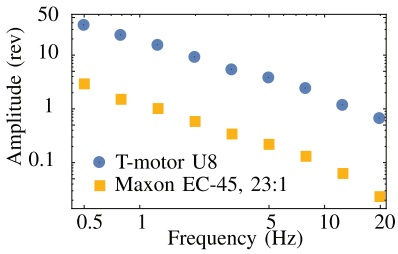

Fig. 6. Bode plot of amplitude response (in revolutions) to sinusoidal voltage input at various frequencies.

TABLE II
PHYSICAL PROPERTIES OF THE MACHINES OF INTEREST (II-C)

Robot	Legs	DOF	L (m)	M (kg)	Mot. (%)	G
Minitaur	4	8	0.2	5	40	N/A
Delta Hopper	1	3	0.2	2.0	38	N/A
Jerboa	2	4	0.105	2.5	40	N/A
MIT Cheetah	4	12	0.275	33	24	5.8
XRL	6	6	0.2	8	11	23
ATRIAS	2	6	0.42	60	11	50
StarlETH	4	12	0.2	23	16	100
Cheetah Cub	4	8	0.069	1	16	300

open-loop sinusoidal voltages at various frequencies, and the amplitude of the output shaft of the motor (in revolutions) was recorded. The U8s performed significantly better at this bandwidth measure, rotating on average 17.4x more than the geared EC45's, as shown in Fig. 6.

D. Relevance to Behaviors

For the 2–5 kg machines in this family, the duration of stance phase is on the order of 0.1 seconds, corresponding (roughly) to a spring-mass time constant of > 5 Hz for each stance leg. This illustrates the importance of having good actuation performance at the time scales depicted in Figure 6.

IV. IMPLEMENTATION AND PERFORMANCE

The basic motor control electrical subsystem of the DD family is described in [5, Section V-A.3], stemming from work reported in [4]. Of additional relevance to this letter is the closed-loop control architecture, which, building on the brushless servo approach of [29] is implemented using fixed-rate 1KHz 16-bit PWM control signals in a master–slave layout. The central "computer" node (STM32F3 microcontroller at 72 MHz) has two communication lines to each motor, namely position (motor→computer) and desired voltage (computer→node). We have found that this somewhat stark implementation has minimal overhead for ease of implementation and re-iteration, and also ensures minimal closed-loop latency (Section III-C and Fig. 6).

A. Performance Metrics

Table II provides physical properties and Table III performance measures for this family of DD robots as well as

TABLE III
PERFORMANCE MEASURES OF THE MACHINES OF INTEREST (II-C)

Robot	v_{ss} (m/s, LL/s)	α_v (m/s)^2	a_{mcv} [DD] (g)	CoT
Minitaur	1.45, 7.25	4.70	0.69	2.3
Delta Hopper	N/A	3.44	0.59	N/A
Jerboa	1.52, 14.5	1.37	0.39	2.5
MIT Cheetah	6, 21.8	4.91	1.33 [−0.60]	0.51
XRL	1.54, 7.7	4.17	1.14 [−0.91]	0.9
ATRIAS	2.53, 6.00	N/A	2.03 [−0.94]	1.46
StarlETH	0.7, 3.5	3.09	0.37 [−0.99]	2.57
Cheetah Cub	1.42, 20.8	0.20	19.38 [−0.93]	9.8

examples of geared machines over a wide range of mass (1-60 kg).[9]

Wherever possible, the maximum experimentally observed forward running **steady velocity** (v_{ss}) of the robots of interest will be provided in m/s, and maximum leg length per second (LL/s) .

Specific agility as defined in [33] represents the "mass-normalized change in extrinsic body energy [during stance]." Motivated by tasks such as ledge ascent, this measure will be restricted, in this context, to jumps that have a significant vertical component, denoted **vertical specific agility** (α_v). Rotational and horizontal translational components of the energy will be assumed negligible, such that

$$\alpha_v = h_{\max} g, \tag{10}$$

where $h_{\max}$ is the maximal experimentally observed vertical jump height of the machine, and g the gravitational constant.

Since specific force is the first limiting resource, a measure is necessary to understand whether a given machine will even be able to support its own weight without thermal damage to the actuators. The leg's infinitesimal kinematics have significant influence; we consider the minimum continuous vertical force that can be exerted by the machine, and normalize by the gravitational force acting on its mass, then subtract one, yielding an estimate of the **minimal continuous vertical acceleration** (a_{mcv}):

$$a_{\text{mcv}} := \frac{\tau_c n_l}{mg} \left(\min_q \Gamma_v(q) \right) - 1 \tag{11}$$

whereby we assume that all legs have sufficient workspace for the links to be parallel. τ_c denotes the thermally sustainable

[9]Here, L is the mean leg length, Mot. is motor mass fraction, M the mass, and G the gear ratio.

For the MIT Cheetah (custom non-COTS motors), motor mass fraction was computed based on the high power actuators only, as the motor mass of the "shape-change" (out of sagittal plane) motors is negligible in comparison, the largest recoverable jump height was from direct correspondence with the author.

The XRL (Maxon EC45, 70W, 23:1) v_{ss} is actually XRHex data [18].

ATRIAS [19] (MF0150010 [24] v_{ss} is from [30], and once again only the high power actuators are considered for the mass fraction.

The StarlETH [31] (Maxon EC4-Pole, 200W, 100:1) jump height was taken from [32] by counting pixels in the jump image since COM displacement was not reported.

The Kondo KRS2350 servos in the Cheetah Cub [21] were assumed to have 1/3 motor mass, and "stall torque" was assumed to correspond to 100 °C rise, and jump height was also determined from discussion with the author.

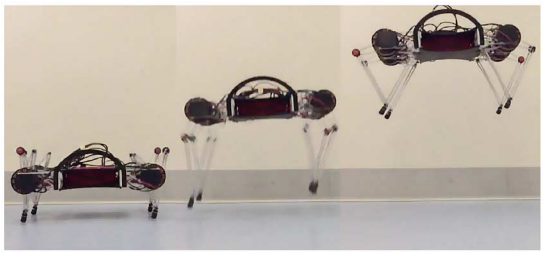

Fig. 7. 48 cm vertical jump of the Minitaur robot.

continuous torque (assumed to be a $100\,^{\circ}C$ rise), and n_l the number of legs that can push vertically. This dimensionless number will indicate if the machine will be able to support its own weight at any point in the leg's workspace (≥ 0), and represents the instantaneous vertical acceleration of the body in units of gravitational constant. For comparisons with other machines, the measure is listed both as designed and also as if the machine's gearbox were removed.

The cost of transport (**specific resistance** [34], [35]) is computed using mean voltage (V) and current (i):

$$CoT := \frac{Vi}{Mgv_{\text{ss}}} \tag{12}$$

B. Performance of the DD Machines

The family of DD machines in this letter performs similarly or better in conventional measures compared to more established, geared, machines. The Minitaur robot has forward running speed (v_{ss}) of $1.45\frac{m}{s}$ for a bound, and $0.8\frac{m}{s}$ for a pronk, competitive for machines around its length scale, and its vertical jump height (represented by α_v, and shown in Fig. 7 is the second best of all the machines considered. The specific resistance of the DD robots is no worse than that of other machines of a similar scale (StarlETH and Cheetah Cub), though the larger machines perform better (as expected). Our machines have proven to be quite robust both mechanically and thermally and have each been run for tens of hours as the gaits were developed. We believe that the true benefits of our DD machines will be realized in tasks that fully exploit the increased proprioception, such as rapid transitions between substrates or locomotion modalities, a topic we leave to future work.

V. Conclusion

This letter outlines a design methodology that brings the well known benefits of DD robotics to legged locomotion. These benefits include significant improvements (3.8x–96x) in the constituent components (reflected inertia, and static, kinetic, and viscous friction) of a simple actuator "transparency" model, as well as a 17.4x improvement in rotational bandwidth as compared to a representative geared motor (Maxon EC45 flat, 23:1). The family of machines built with these actuators in accordance with the design principles listed above has proven very competitive with state of the art legged machines, according to a variety of metrics. The diversity of morphologies and similarly competitive running and leaping gaits exhibited by the family of machines we describe suggests that DD legged locomotion may be more readily achievable than its very sparse literature hitherto might suggest.

Work currently in progress addresses a number of important questions concerning the role of form and function that lies beyond the scope of the present design-focused letter. Careful study will be required to tease out the relative contributions to overall energetic efficiency due to DD–both advantages and disadvantages–as distinct from the control policies they enable. In addition to the convincing and tunable compliance that DD affords, these machines do not preclude integration of passive, purely mechanical, compliance elements. From the morphological perspective, the analysis of framing cost, in Section II-E suggests an approach to actuator granularity that might help rationalize decisions as to how many appendages of a number of DOF a robot might requires to achieve a specified domain of tasks.

We believe we have merely scratched the surface in extracting the benefits of "transparency" that DD actuation offers legged robotics. The high sensorimotor bandwidth enjoyed by these machines greatly facilitates simple reactive strategies, affording, for example, reliable observer-free proprioceptive touchdown detection (cf. [36]). In turn, bringing such high sensing and control authority to bear upon platforms whose dynamics are so well described by simple hybrid Lagrangian mechanics [22] facilitates the application and reuse of simple, robust behavioral "modules" whose parallel [37] and sequential [38] compositions can now be extended across multiple bodies as well as flexibly recombined within a single one. Work in progress further exploits these machines' ability to "feel" their environment in bringing the perspective of "self-manipulation" [22] to bear on legged mobility, especially as it relates to transitional behavior.

Appendix

A. Invariance of Leg Design Measures to Leg Angle

For each of the leg designs, there is a linear change of coordinates $L : T^2 \to T^2$ from the original joint angles such that if $\alpha = Lq$, then α_1 is the "leg angle," i.e.

$$g(q) = \widetilde{g}(Lq), \qquad \widetilde{g}(\alpha) = \mathrm{R}(\alpha_1)h(\alpha_2). \tag{13}$$

For the serial design (3), $L_{\mathrm{S}} = I$, and for each of the parallel designs (4)–(5), $L_{\mathrm{P}} := \frac{1}{2}\left[\begin{smallmatrix} 1 & 1 \\ 1 & -1 \end{smallmatrix}\right]$.

Proposition 1: The singular values of the Jacobian of (13), $\mathrm{D}g$, are invariant to the leg angle, α_1.

Proof: At first, we show that if $L = I$, the proposition holds:

Using the chain rule on (13),

$$\mathrm{D}g = S\mathrm{R}he_1^T + \mathrm{RD}h, \tag{14}$$

where we drop the dependencies $\mathrm{R}(\alpha_1)$, $h(\alpha_2)$ and $\mathrm{D}h(\alpha_2)$ for brevity, $S := \left[\begin{smallmatrix} 0 & -1 \\ 1 & 0 \end{smallmatrix}\right]$, and $e_1 := \left[\begin{smallmatrix} 1 \\ 0 \end{smallmatrix}\right]$. Now, multiplying and simplifying (14),

$$\mathrm{D}g^T\mathrm{D}g = \mathrm{D}h^T\mathrm{D}h + e_1h^The_1 + \mathrm{D}h^TShe_1^T + e_1h^TS^T\mathrm{D}h,$$

and observe that all dependence on α_1 (in the form of R in (14)) disappears. Thus, $\mathrm{D}g^T\mathrm{D}g$ is invariant to α_1.

Lastly, since $\mathrm{D}L = L$ is constant, and

$$\mathrm{D}g^T \mathrm{D}g = L^T \mathrm{D}\widetilde{g}^T \mathrm{D}\widetilde{g} L, \tag{15}$$

the linear coordinate change L does not affect this proposition, and the argument above for $L = I$ carries over directly. □

B. Relation of Measures to Jacobian Singular Values

Let the (ordered) singular values of the square matrix J be $\{\sigma_{\max}, \sigma_{\min}\}$. Observe that

1) The expression on the left hand side of (8) is the Rayleigh quotient for the matrix JJ^T, which is minimized by its smallest eigenvalue [39]. Additionally, J^T and J have the same singular values, and so any measure depending on the singular values of J or of J^T is invariant to leg angle (Appendix A).
2) Since the eigenvalues of $(J^T J)^{-1}$ are the reciprocals of eigenvalues of $J^T J$, the singular values of J appear in the denominator of (9).
3) Since $\mathrm{trace}(JJ^T) = \mathrm{trace}(J^T J)$, the Asada metric of II-B3 is also independent of leg angle.

ACKNOWLEDGEMENTS

The authors would like to thank Jeff Duperret for the Bode plot code.

REFERENCES

[1] H. Asada and K. Youcef-Toumi, *Direct-Drive Robots: Theory and Practice*. Cambridge, MA, USA: MIT Press, 1987.
[2] Y. Sakagami, R. Watanabe, C. Aoyama, S. Matsunaga, N. Higaki, and K. Fujimura, "The intelligent ASIMO: System overview and integration," in *Proc. IEEE/RSJ Int. Conf. Intell. Robots Syst.*, 2002 vol. 3, pp. 2478–2483.
[3] G. A. Pratt and M. M. Williamson, "Series elastic actuators," in *Proc. IEEE Int. Conf. Intell. Robots Syst.*, 1995, vol. 1, pp. 399–406.
[4] G. Kenneally, A. De, and D. E. Koditschek, "Design principles for a family of direct-drive legged robots," in *Proc. Robot. Sci. Syst. Workshop*, 2015.
[5] A. De and D. E. Koditschek, "The Penn Jerboa: A platform for exploring parallel composition of templates," arXiv preprint arXiv:1502.05347, 2015.
[6] J. W. Hurst, "The role and implementation of compliance in legged locomotion," Ph.D. dissertation, Robotics Institute, Carnegie Mellon Univ., Pittsburgh, PA, USA, Aug. 2008.
[7] M. Motors. (2014). "Maxon catalog," [Online]. Available: www. maxonmotorusa.com/
[8] A. Wang and S. Kim, "Directional efficiency in geared transmissions: Characterization of backdrivability towards improved proprioceptive control," in *Proc. IEEE Int. Conf. Robot. Autom. (ICRA)*, May 2015, pp. 1055–1062.
[9] S. Seok, A. Wang, D. Otten, and S. Kim, "Actuator design for high force proprioceptive control in fast legged locomotion," in *Proc. IEEE Int. Conf. Intell. Robots Syst.*, 2012 pp. 1970–1975.
[10] N. Hogan, "Impedance control: An approach to manipulation—Part I: Theory," *Trans. ASMEJ. Dyn. Syst. Meas. Control*, vol. 107, no. 1, pp. 1–7, 1985.
[11] M. H. Raibert *et al.*, *Legged Robots That Balance*. Cambridge, MA, USA: MIT Press, 1986 vol. 3.
[12] D. E. Koditschek, "Some applications of natural motion control," *J. Dyn. Syst. Meas. Control*, vol. 113, p. 552, 1991.
[13] C. Loughlin *et al.*, "The DLR lightweight robot: Design and control concepts for robots in human environments," *Ind. Robot Int. J.*, vol. 34, no. 5, pp. 376–385, 2007.
[14] A. J. Spence, S. Revzen, J. Seipel, C. Mullens, and R. J. Full, "Insects running on elastic surfaces," *J. Exp. Biol.*, vol. 213, no. 11, pp. 1907–1920, 2010.
[15] R. S. Wallace, "Miniature direct drive rotary actuators—Part II: Eye, finger and leg," in *Proc. IEEE Int. Conf. Robot. Autom.*, 1994, pp. 1496–1501.
[16] B. Na, H. Choi, and K. Kong, "Design of a direct-driven linear actuator for a high-speed quadruped robot, Cheetaroid-I," *IEEE/ASME Trans. Mechatron.*, vol. 20, no. 2, pp. 924–933, Apr. 2015.
[17] G. Kenneally and D. E. Koditschek, "Leg design for energy management in an electromechanical robot," in *Proc. IEEE/RSJ Int. Conf. Intell. Robots Syst.*, 2015, pp. 5712–5718.
[18] K. C. Galloway *et al.*, "X-RHex: A highly mobile hexapedal robot for sensorimotor tasks," Univ. Pennsylvania, Philadelphia, PA, USA, Tech. Rep., 2010.
[19] J. Grimes and J. Hurst, "The design of ATRIAS 1.0 a unique monopod, hopping robot," in *Proc. Adapt. Mobile Robot./15th Int. Conf. Climbing Walking Robots Support Technol. Mobile Mach. (CLAWAR'12)*, 2012, pp. 548–554.
[20] M. Hutter, C. Remy, M. Hoepflinger, and R. Siegwart, "Efficient and versatile locomotion with highly compliant legs," *IEEE/ASME Trans. Mechatron.*, vol. 18, no. 2, pp. 449–458, Apr. 2013.
[21] A. Sprowitz, A. Tuleu, M. Vespignani, M. Ajallooeian, E. Badri, and A. J. Ijspeert, "Towards dynamic trot gait locomotion: Design, control, and experiments with Cheetah-cub, a compliant quadruped robot," *Int. J. Robot. Res.*, vol. 32, pp. 932–950, 2013.
[22] A. Johnson and D. Koditschek, "Legged self-manipulation," *IEEE Access*, vol. 1, pp. 310–334, May 2013.
[23] *T-Motor U8 Datasheet* [Online]. Available: www.rctigermotor.com/
[24] *Allied Motion Datasheet* [Online]. Available: www.alliedmotion.com/
[25] *Uu Motor Datasheet* [Online]. Available: www.uumotor.com/
[26] S. Seok, A. Wang, M. Chuah, D. Otten, J. Lang, and S. Kim, "Design principles for highly efficient quadrupeds and implementation on the MIT Cheetah robot," in *Proc. IEEE Int. Conf. Robot. Autom.*, 2013, pp. 3307–3312.
[27] H. Rad, P. Gregori, and M. Buehler, "Design, modeling and control of a hopping robot," in *Proc. Int. Conf. Intell. Robots Syst.*, 1993, pp. 1778–1785.
[28] R. M. Murray, Z. Li, S. S. Sastry, and S. S. Sastry, *A Mathematical Introduction to Robotic Manipulation*. Boca Raton, FL, USA: CRC Press, 1994.
[29] M. Piccoli and M. Yim, "Anticogging: Torque ripple suppression, modeling, and parameter selection," *Int. J. Robot. Res.*, vol. 35, no. 1–3, pp. 148–160, 2016.
[30] *ATRIAS Robot: 9.1 Kph Running Speed (5.7 Mph)* [Online]. Available: www.youtube.com/watch?v=U4eBRPHYCdA
[31] M. Hutter, C. Gehring, M. Bloesch, M. Hoepflinger, C. Remy, and R. Siegwart, "StarlETH: A compliant quadrupedal robot for fast, efficient, and versatile locomotion," in *Proc. Adapt. Mobile Robot./15th Int. Conf. Climbing Walking Robots Support Technol. Mobile Mach. (CLAWAR'12)*, 2012, pp. 483–490.
[32] C. Gehring, S. Coros, M. Hutter, and R. Siegwart, "An optimization approach to controlling jump maneuvers for a quadruped robot," in *Proc. Conf. Dyn. Walking*, 2015.
[33] J. M. Duperret, G. D. Kenneally, J. L. Pusey, and D. E. Koditschek, "Towards a comparative measure of legged agility," in *Proc. Int. Symp. Exp. Robot.*, Jun. 2014, pp. 3–16.
[34] M. Ahmadi and M. Buehler, "The ARL Monopod II running robot: Control and energetics," in *Proc. IEEE Int. Conf. Robot. Autom.*, 1999, vol. 3, pp. 1689–1694.
[35] G. Gabrielli and T. von Karman, "What price speed?" *Mech. Eng.*, vol. 72, pp. 775–781, 1950.
[36] A. Johnson, G. Haynes, and D. Koditschek, "Disturbance detection, identification, and recovery by gait transition in legged robots," in *Proc. IEEE/RSJ Int. Conf. Intell. Robots Syst. (IROS'10)*, 2010, pp. 5347–5353.
[37] A. De and D. Koditschek, "Parallel composition of templates for tail-energized planar hopping," in *Proc. IEEE Int. Conf. Robot. Autom.*, 2015, pp. 4562–4569.
[38] A. L. Brill, A. De, A. M. Johnson, and D. E. Koditschek, "Tail-assisted rigid and compliant legged leaping," in *Proc. IEEE/RSJ Int. Conf. Intell. Robots Syst.*, 2015, pp. 6304–6311.
[39] R. Horn and C. Johnson, *Matrix Analysis*. Cambridge, U.K.: Cambridge Univ. Press, 1990.